Spring 2024

Development of On-The-Fly Quasi-Steady State Approximation for Chemical Kinetics in CFD

Abhinav Balamurugan
Embry-Riddle Aeronautical University, balamura@my.erau.edu

By

A Thesis Submitted to the Faculty of Embry-Riddle Aeronautical University

In Partial Fulfillment of the Requirements for the Degree of

Master of Science in Aerospace Engineering

Embry-Riddle Aeronautical University

Daytona Beach, Florida

By

THESIS COMMITTEE

Graduate Program Coordinator, Dr. Hever Moncayo	Date
Dean of the College of Engineering, Dr. James W. Gregory	Date
Associate Provost of Academic Support, Dr. Kelly Austin	Date

ACKNOWLEDGMENTS

I extend my deepest gratitude to my advisor, Dr. Eric Perrell, for his support, guidance, and invaluable insights throughout the course of this research. His expertise and encouragement have been pivotal to my development and the completion of this thesis.

I am also immensely thankful to my committee members, Dr. William Engblom, Dr. Scott Martin, and Dr. Laksh Narayanaswami, whose feedback and criticism have significantly enriched this work. Their perspectives have been instrumental in shaping the outcome of this research and me as a engineer.

Special thanks go to Spencer Moore for his collaboration, stimulating discussions, and the sharing of ideas that have greatly enhanced my research experience.

This thesis represents not just my work, but the support and guidance I've received along the way. To everyone involved, thank you for your invaluable contributions and for being part of this journey.

ABSTRACT

This study analyzes the feasibility of On-The-Fly Quasi-Steady-State Approximation (OTF-QSSA) applicaiton for solving chemical kinetics within Computational Fluid Dynamics (CFD) simulations, aiming to reduce the computational demand of detailed mechanisms. An algorithm that dynamically identifies and designates Quasi-Steady-State (QSS) species at specific grid locations and instances during the simulation was developed. With this information, our method pseudo-delays the advancement of concentrations for these QSS species—effectively setting their rate of concentration change to zero for a set number iteration before updating using the detailed mechanism and thereby omitting the computationally intensive processes typically required for their calculation during those skipped iteration. This strategy intends to demonstrate computational time savings at the cost of minimal accuracy loss.

To evaluate the effectiveness of OTF-QSSA, we conducted a series of tests on a 1D channel flow model simulating hydrogen and air combustion, utilizing the Evans & Schexnayder 25 reaction-12 species chemistry model alongside two derived models: an 8 reaction-7 species model commonly used in the community, and a 16 reaction-8 species model. The findings indicate that OTF-QSSA in simple scenarios, such as the 8 reaction model showed poorer performance, most likely due to the overhead of implementing OTF-QSSA outweighing the potential time savings. However, the approach yields significant efficiency improvements in more complex cases such as the 16-reaction and the full 25-reaction model with the 25 reaction model showing a system time reduction of approximately 15.59%. This reduction in computational time was achieved with minimal impact on the accuracy of major species concentrations, though some minor species, specifically the nitrogen based species, did exhibit slight deviations which did not substantially affect the overall simulation outcomes.

The implications of these findings suggest a promising avenue for reducing computational demands in modeling detailed chemical reactions, enabling better efficient and practical simulations in combustion and other areas of fluid dynamics.

TABLE OF CONTENTS

ACKNOWLEDGMENTS **i**

ABSTRACT **ii**

LIST OF FIGURES **vii**

LIST OF TABLES **viii**

NOMENCLATURE **ix**

1 Introduction **1**

1.1 Chemical Kinetics Review 1

1.1.1 Quasi-Steady State Assumption 3

1.2 Objectives of Study 4

1.2.1 Definition of OTF-QSSA 4

2 Relevant Literature **5**

3 Methodology **7**

3.1 OTF-QSSA Numerical Approach 7

3.1.1 Algorithm User Constraints 8

3.1.2 Step-by-Step Procedure 9

3.1.3 QSS Species Selection 10

3.1.4 Global Adaptive Time Stepping 10

3.2 HYP Code 11

4 Verification **12**

4.1 Chemistry Modelling 12

4.2 Pre-mixed 1D-Channel Flow 15

5 Results and Discussion **17**

5.1 Case 1: Evans and Schexnayder 7 Species - 8 Reactions 17

5.2 Case 2: Evans and Schexnayder 8 Species - 16 Reactions 22

5.3 Case 3: Evans and Schexnayder 12 Species - 25 Reactions 26

6 Conclusion **34**

6.1 Remarks 34

6.2 Limitation of the Current Model 34

REFERENCES **36**

LIST OF FIGURES

Figure **Page**

3.1 QSSA Implementation Visualization 7

3.2 OTF-QSSA Iteration Visualization 7

4.1 1D Channel Grid 15

5.1 Evans and Schexnayder 7 Species - 8 Reactions Model: Major Species Mass Fractions (Dashed Lines - Without QSSA, Solid Line - With QSSA) 18

5.2 Evans and Schexnayder 7 Species - 8 Reactions Model: Minor Species Mass Fractions (Dashed Lines - Without QSSA, Solid Line - With QSSA) 18

5.3 Evans and Schexnayder 7 Species - 8 Reactions Model: Temperature Dashed Lines - Without QSSA, Solid Line - With QSSA) 19

5.4 Evans and Schexnayder 7 Species - 8 Reactions Model: Pressure (Dashed Lines - Without QSSA, Solid Line - With QSSA) 19

5.5 Evans and Schexnayder 7 Species - 8 Reactions Model: X-Velocity (Dashed Lines - Without QSSA, Solid Line - With QSSA) 20

5.6 Evans and Schexnayder 7 Species - 8 Reactions Model: RRMSE Of Composition (Dashed Lines - Without QSSA, Solid Line - With QSSA) 20

5.7 Evans and Schexnayder 7 Species - 8 Reactions Model: RRMSE Of State and Velocity (Dashed Lines - Without QSSA, Solid Line - With QSSA) 21

5.8 Evans and Schexnayder 7 Species - 8 Reactions Model: Average Number of QSS Species per grid cell 21

5.9 Evans and Schexnayder 8 Species - 16 Reactions Model: Major Species Mass Fractions (Dashed Lines - Without QSSA, Solid Line - With QSSA) 23

5.10 Evans and Schexnayder 8 Species - 16 Reactions Model: Minor Species Mass Fractions (Dashed Lines - Without QSSA, Solid Line - With QSSA) 23

5.11 Evans and Schexnayder 8 Species - 16 Reactions Model: Temperature (Dashed Lines - Without QSSA, Solid Line - With QSSA) 24

5.12 Evans and Schexnayder 8 Species - 16 Reactions Model: Pressure (Dashed Lines - Without QSSA, Solid Line - With QSSA) 24

5.13 Evans and Schexnayder 8 Species - 16 Reactions Model: X-Velocity (Dashed Lines - Without QSSA, Solid Line - With QSSA) 25

5.14 Evans and Schexnayder 8 Species - 16 Reactions Model: Average Number of QSS Species per grid cell 25

5.15 Evans and Schexnayder 12 Species - 25 Reactions Model: Major Species Mass Fractions *(Delta - Without QSSA, Dashed Lines - QSSA Case a, Solid Line - With QSSA Case b)* 27

5.16 Evans and Schexnayder 12 Species - 25 Reactions Model: Minor Species (Excluding Nitrogen Based Species) Mass Fractions (Delta - Without QSSA, Dashed Lines - QSSA Case a, Solid Line - With QSSA Case b) 27

5.17 Evans and Schexnayder 12 Species - 25 Reactions Model: Minor Nitrogen Based Species Mass Fractions (Delta - Without QSSA, Dashed Lines - QSSA Case a, Solid Line - With QSSA Case b) 28

5.18 Evans and Schexnayder 12 Species - 25 Reactions Model: RRMSE (%) Major-Minor Species (Excluding Nitrogen Based Species) 29

5.19 Evans and Schexnayder 12 Species - 25 Reactions Model: RRMSE (%) Major-Minor Species *(Excluding Nitrogen Based Species)* Mass Fractions with OTF-QSSA Enabled at 80^{th} Grid Cell 29

5.20 Evans and Schexnayder 12 Species - 25 Reactions Model: RRMSE (%) Nitrogen Based Trace Species Mass Fractions with OTF-QSSA Enabled at 1^{st} Grid Cell 30

5.21 Evans and Schexnayder 12 Species - 25 Reactions Model: RRMSE (%) Nitrogen Based Trace Species Mass Fractions with OTF-QSSA Enabled at 80^{th} Grid Cell 30

5.22 Evans and Schexnayder 12 Species - 25 Reactions Model: RRMSE (%) Of State and Velocity with OTF-QSSA Enabled at 1^{st} Grid Cell 31

5.23 Evans and Schexnayder 12 Species - 25 Reactions Model: RRMSE (%) Of State and Velocity with OTF-QSSA Enabled at 80^{th} Grid Cell 31

5.24 Evans and Schexnayder 12 Species - 25 Reactions Model: Temperature (Delta - Without QSSA, Dashed Lines - QSSA Case a, Solid Line - With QSSA Case b) 32

5.25 Evans and Schexnayder 12 Species - 25 Reactions Model: Pressure (Delta - Without QSSA, Dashed Lines - QSSA Case a, Solid Line - With QSSA Case b) 32

5.26 Evans and Schexnayder 12 Species - 25 Reactions Model: Velocity (Delta - Without QSSA, Dashed Lines - QSSA Case a, Solid Line - With QSSA Case b) 33

5.27 Evans and Schexnayder 12 Species - 25 Reactions Model: Average Number of QSS Species at a grid cell 33

LIST OF TABLES

Table		Page
4.1	Evans and Schexnayder Hydrogen Air Reaction Model [1]	12
4.2	Reaction Set and their Species	15
4.3	Inflow Species Mass Fractions	16
4.4	Inflow Conditions	16
5.1	User Constraints: Evans and Schexnayder 8 Reactions Model	17
5.2	User Constraints: Evans and Schexnayder 16 Reactions Model	22
5.3	User Constraints: Evans and Schexnayder 25 Reactions Model	26

NOMENCLATURE

ΔG_T^0	Standard-State Gibbs Function Change
$\dot{\omega}$	Rate of Concentration Change
ϵ_c	QSS Check Count
ϵ_s	QSS Store Count
ϵ_u	Concentration Update Count
η	QSS Relaxation Factor
ν	Stoichiometric Coefficient
ζ	Time Step Relaxation Factor
g_f^0	Gibbs Function of Formation
A	Pre-exponent Coefficient
C, [ ]	Species Concentration
E_A	Activation Energy
k	Reaction Rate Coefficient
K_c	Equilibrium Constant-Concentration Based
K_p	Equilibrium Constant-Pressure Based
L	Loss Terms from the Rate Equation
N	Number of (Species or Reactions)
n	Temperature Exponent

P Production Terms from the Rate Equation

R_u Universal Gas Constant

T Temperature

SUBSCRIPTS

b Backward

f Forward

i i^{th} Reaction

j j^{th} Specie

log Relative Rate of Concentration Change in logarithmic scale

max Maximum Relative Rate of Concentration Change in logarithmic scale

r Reactions

rel Relative Rate of Concentration Change

s Species

small Smallest Positive Rate of Concentration Change

SUPERSCRIPTS

' Reactant

" Product

ACRONYMS

CFD Computational Fluid Dynamics

CFL Courant–Friedrichs–Lewy Condition

DCK Detailed Chemical Kinetics

OTF On-The-Fly

QSS Quasi-Steady State

QSSA Quasi-Steady State Approximation/ Assumption

1 Introduction

Computational Fluid Dynamics (CFD) integrated with chemical kinetics offers a powerful tool for simulating the complex interactions between fluid flow and chemical reactions. This interdisciplinary approach is critical in a wide range of applications, from analyzing propulsion systems to hypersonic flows. However, the integration of detailed chemical kinetics into CFD simulations is computationally intensive, requiring significant processing power and time due to the complexity and the large number of species and reactions involved.

To manage these computational demands, various simplification methods have been developed. These methods aim to reduce the complexity of the chemical kinetics involved without significantly compromising the accuracy of the simulations. A few examples include the Global reaction equation, where the entire reaction set is simplified to only involve the major species. This is sufficient for most simple engineering processes but usually doesn't provide the full physics behind the chemical system. To improve upon this, there are multiple-equation models which include some intermediary species to obtain better resolution on the results.

A couple of other methods include Partial Equilibrium, wherein certain reactions are assumed to be in a equilibrium state with the other reactions being integrated. The Quasi-Steady-State Assumption (QSSA) assumes that certain species reach a steady state rapidly, meaning their rate of concentration change is minimal, compared to others, QSSA reduces the computational need to solve some reaction mechanism, thus reducing the overall computational load.

1.1 Chemical Kinetics Review

Chemical kinetics focuses on understanding how fast chemical reactions occur and the factors that affect these rates. The Rate Equation, outlined in Equation (1.1), provides a method for calculating these rates using the concentrations, C or [ ], of the participating species and some basic information about the reaction itself, such as reaction rate coefficients, k_f and k_b, and stoichiometric coefficients, ν. For illustration purpose, assume a reaction set

given by Equation (1.2). The rate of concentration change of species Z, $\dot{\omega}_Z$, can be calculated using Equation (1.3)

$$\dot{\omega_j} = \sum_{i=1}^{N_r} \nu_{ji} q_i \quad for \quad j = 1, 2, ..., N_s \tag{1.1a}$$

where

$$\nu_{ji} = \left(\nu_{ji}^{''} - \nu_{ji}^{'}\right) \tag{1.1b}$$

and

$$q_i = k_{fi} \prod_{j=1}^{N_s} C_j^{\nu_{ji}^{'}} - k_{bi} \prod_{j=1}^{N_s} C_j^{\nu_{ji}^{''}} \tag{1.1c}$$

$$Reaction \quad 1 : X + Y \longleftrightarrow Z \tag{1.2a}$$

$$Reaction \quad 2 : 2Z \longleftrightarrow W \tag{1.2b}$$

$$\frac{d[Z]}{dt} = \dot{\omega}_Z = k_{f1}[X][Y] - k_{b1}[Z] - 2k_{f2}[Z]^2 + 2k_{b2}[W] \tag{1.3}$$

The Arrhenius equation is commonly used to calculate these rate coefficients from experimental data. The general form is given in Equation (1.4), where A is the pre-exponential coefficient, n being the temperature exponent, and E_A being the activation energy.

$$k_{fi} = A_{fi} T^{n_{fi}} e^{\frac{-E_{A_{fi}}}{R_u T}} \tag{1.4a}$$

and

$$k_{bi} = A_{bi} T^{n_{ri}} e^{\frac{-E_{A_{bi}}}{R_u T}} \tag{1.4b}$$

Another approach for calculating backward rates, given the forward rates, involves the use of Gibbs Energy of Formation, detailed in Equation 1.5. This method begins by calculating the equilibrium constant using the Gibbs Energy of Formation for the reaction and then derives the backward rate coefficient using the forward rate coefficient as formulated in Equation (1.5). Understanding both forward and backward reaction rates is important for predicting the overall reaction rates and is essential for accurately determining species mass fractions

as the reaction progresses. For more in depth understanding refer to these texts, *Principles of Combusiton* by *Kenneth K. Kuo* [2] and *An Introduction to Combustion: Concepts and Applications* by *Stephen Turns* [3].

$$\Delta G^0_{Ti} = \sum_{j=1}^{N_s} \nu_{ji} \bar{g}^0_f \tag{1.5a}$$

$$K_{pi} = e^{-\frac{\Delta G^0_{Ti}}{R_u T}} \tag{1.5b}$$

$$K_{ci} = \frac{K_{pi}}{(RT)^{\Delta \nu_i}} \tag{1.5c}$$

where

$$\Delta \nu_i = \sum_{j=1}^{N_s} \nu_{ji} \tag{1.5d}$$

$$K_{ri} = \frac{K_{fi}}{K_{ci}} \tag{1.5e}$$

1.1.1 Quasi-Steady State Assumption

The QSSA in chemical kinetics is a reduced approach used to analyze complex reaction mechanisms involving multiple reaction sets and species. It is based on the premise that certain reactive intermediates or radical species reach a steady-state concentration early in the reaction process, even though the system as a whole has not yet reached equilibrium. By assuming that the rate of concentration change of these intermediates, or Quasi-Steady State (QSS) species, is negligible over certain time periods, the QSSA effectively decouples their behavior from the overall chemical dynamics of the system. An approach for using QSSA would be to set Equation (1.1a) to a value of zero and the new rates of QSS Species are identified by solving a system of equations. Turns [3] uses another approach by first differentiating Equation (1.1) and then setting the second order rate change of QSS species to a value of zero. This derived set of equations are then used to obtain the rate change of QSS species. The non-QSS species rates are simply calculated by integrating Equation (1.1). While this method seems straightforward, there is an inherent difficulty in predicting species behavior without prior knowledge and the trade off for implementing this in CFD

solvers is still unknown as the rates changes of those QSS species might still be substantial and may force the equations to remain stiff.

1.2 Objectives of Study

The objectives of this study is to develop and verify an on-the-fly QSSA (OTF-QSSA) algorithm to reduce the computational workload of chemical kinetics in CFD.

1.2.1 Definition of OTF-QSSA

On-the-fly QSSA dynamically identifies Quasi-Steady State (QSS) species during the progression of reactions, unlike traditional static approaches. It continuously assesses reaction rates, adding or removing species from the QSS list based on their local rates. This method adapts to changes in the reaction the as reaction progresses, both in time and space.

2 Relevant Literature

Zhang et al. [4] present a novel approach to kinetic mechanism reduction, combining on-the-fly reduction and the Quasi-Steady-State Approximation (QSSA). Their methodology integrates dynamic and global reduction techniques. A set of global QSS species are selected and the dynamic reduction, based on instantaneous fluxes, updates that list on-the-fly. The QSS specie' concentrations are then solved using an algebraic non-linear equation solver and the non-QSS specie' concentrations are integrated through the chemical rate equations.

The QSSA scheme, used by Verwer and Simpson [5], is a straightforward approach for solving QSS specie' concentrations, given in Equation 2.2, under the assumption that production (P) and loss (L) terms for QSS species in the chemical kinetics equations are slowly varying. Equation (2.1) shows how P and L are derived from the rate Equation (1.1).

This method has a lower computational workload per time step, similar to low-stage explicit Runge-Kutta methods work and is generally cheaper to run in comparison to general purpose stiff ODE solvers. A modified QSSA method extends it by using a two-stage integration process relying on lumping of reactions to reduce the mechanism and tuning error checkers specific to the chemical model to achieve second-order accuracy.

$$X + Y \longrightarrow Z \tag{2.1a}$$

$$P_Z = kf[X][Y] \tag{2.1b}$$

$$L_Z = \frac{kb[Z]}{[Z]} \tag{2.1c}$$

$$C(t + \Delta t) \approx e^{-\Delta t L} C(t) + \left(1 - e^{-\Delta t L}\right) \frac{P}{L} \tag{2.2}$$

Verwer and Simpson's [5] analysis demonstrates the potential for QSSA methods to achieve considerable computational efficiency in modeling atmospheric chemical kinetics, especially when properly tuned and adapted to the chemistry involved.

Mott et al. [6] present a unique QSS method for integrating the stiff differential equations in reaction kinetics. It is predictor–corrector scheme with additional time corrective coeffi-

cients, known for its second-order accuracy and adaptability across various species regardless of their individual time scales. The α-QSS algorithm is a derivation of the exact solution of simplified reaction kinetics equations under the assumption of constant reaction rates, Equation (2.3). The algorithm uses a mixture of initial and predicted values to average the production and loss terms from the rate equation, with α serving as an additional corrective factor based on the weighted average of L, as defined in Equation (2.4).

$$C(\Delta t) = C^0 + \frac{\Delta t(P - LC^0)}{1 + \alpha L \Delta t} \tag{2.3}$$

where

$$\alpha(L\Delta t) \equiv \frac{1 - \frac{(1-e^{-L\Delta t})}{L\Delta t}}{1 - (1 - e^{-L\Delta t})} \tag{2.4}$$

Lu and Law's [7] work introduces a unique method for obtaining analytic solutions for the concentrations of QSS species, leveraging a blend of linear approximations and graph theory. Recognizing the limitations imposed by nonlinear algebraic equations in determining QSS species concentrations, Lu and Law [7] propose linearizing these equations to simplify their resolution. This linearization process, termed LQSSA, approximates the nonlinear algebraic equations governing QSS species concentrations with a set of linear equations. The linearization is justified on the basis that concentrations of QSS species are typically low, rendering the probability of collisions between two QSS species negligible. The linearized equations are then mapped onto a directed graph, QSSG, obtained from the dependencies among QSS species. This graph-based approach systematically identifies groups of strongly connected QSS species and the inter-dependencies between these groups. This method shows significant improvements in the efficiency and applicability of QSS-based reduced mechanisms in simulations, particularly those involving auto-ignition and perfectly stirred reactors.

For all of the above work, either model-specific reductions such as reaction lumping or approximations from statistical data were needed or involved the use of computational expensive ODE solvers for solving for QSS specie' concentrations. Both of these are difficult to implement in a CFD solver.

3 Methodology

The methodology utilizes the HYP CFD code for studying chemical reaction dynamics through the QSSA. Initially, it identifies QSS species based on criteria set by the user.These species are used in the implementation of QSSA, where their rate of concentration change is maintained at zero for a sequence of user-specified iterations. Figure 3.1 shows how the QSS species concentrations are only updated every n iteration, or time steps, compared to the non-QSS species whose concentrations are updated every iteration.

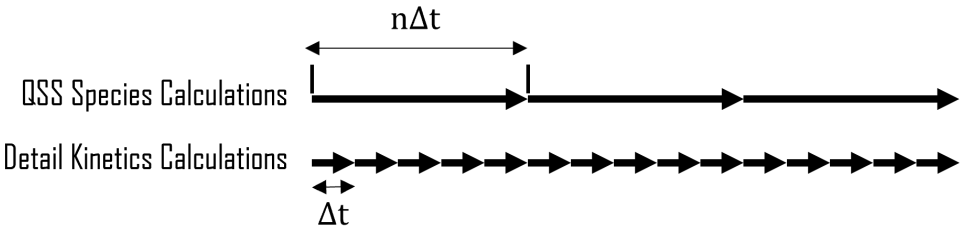

Figure 3.1 QSSA Implementation Visualization

3.1 OTF-QSSA Numerical Approach

The approach is straightforward. The QSS species rate of concentration change is not calculated for all iterations while the non-QSS species are. This "pseudo-delay" tactic would allow the program to skip the processes that involve calculating the rate changes for those QSS species, as represented in figure 3.2. However, to properly implement this concept while maintaining the integrity of the results, some constraints need to be defined. This is further discussed in section 3.1.1.

Base Iteration Counter	1	2	3	4	5	6	7	8	9
QSS Update Iteration Counter	1	2	3	1	2	3	1	2	3
QSS Check Iteration Counter	1			2			3		

Figure 3.2 OTF-QSSA Iteration Visualization

3.1.1 Algorithm User Constraints

To optimize the performance of the QSS algorithm, users need to adjust certain parameters such as those listed below. These adjustments influence how strictly or flexibly the algorithm operates.

QSS Relaxation Factor

Selection of QSS species, η, is governed by a value ranging from 0 to 1, dictating the level of strictness or leniency in identifying these species. A value of 0 indicates that no species are considered as QSS, whereas a value of 1 suggests that all but one species are deemed as QSS.

Concentration Update Count (ϵ_u)

The program utilizes a specified number of iterations to calculate the rate of concentrations change in species using the QSS sequence before it updates these calculations with the rate equation. For the sample pattern shown in figure 3.2, the ϵ_u value would be 3.

QSS Check Count (ϵ_c)

The frequency at which the QSS concentration updating sequence happens before the program checks for new QSS species. For the sample pattern shown in figure 3.2, the concentration updating sequence is performed three times before checking for new QSS species, hence the ϵ_c value would be 3.

QSS Store Count (ϵ_s)

The number of historical "useful/non-zero" rate of concentration change in species that needs to be stored for identifying QSS species. The values stored are replaced in a first-in-first out method.

Time Step Relaxation Factor

The Time Step Relaxation Factor, ζ, modifies the calculated maximum time step in Equation (3.5) to prevent complete depletion species' concentrations.

3.1.2 Step-by-Step Procedure

To grasp the concept of implementing OTF-QSSA, the following enumeration provides a step-by-step process followed by the program.

1. Initially the OTF-QSSA is disabled and the detailed chemical kinetics 1.1 is run for all species.
2. Record rates for all species for ϵ_s iterations.
3. Enable OTF-QSSA.
4. Identify QSS Species according to Equations (3.1), 3.2 and (3.3).
   (a) Determine $\dot{\omega}_s mall$, the smallest non-zero rate among all species j, Equation. (3.2)
   (b) For each species j, compute a "relative rate," defined as the common log of its rate normalized by $\dot{\omega}_s mall$. This is the difference in order of magnitude between each species rate, and the smallest overall rate, Equation (3.1).
   (c) The greatest of these relative rates times a QSS Relaxation Factor η, is the threshold for applying QSS, Equation (3.3).
5. Hold rate of concentration change of QSS species to be zero for ϵ_u iterations. Non-QSS species rates are integrated using detailed kinetics.
6. Calculate a new rate of concentration change of all species, using the detailed mechanism.
7. Repeat steps 5 and 6 for ϵ_c sequence.
8. Recalculate rate changes of all the species by the detailed mechanism.
9. Repeat step 4 to determine a new set of QSS.
10. Repeat steps 5 through 9 until convergence or other user defined stoppages.

3.1.3 QSS Species Selection

The QSS Selection Algorithm calculates the relative rate of change in species concentrations by using a predefined number of past rate changes, determined by the QSS Store Count (ϵ_s). The smallest absolute value of those rate changes is identified as $\dot{\omega}_{small}$ using Equation (3.2). $\dot{\omega}_{small}$ is then used to divide the absolute values of rate of concentration change for each species, as shown in Equation (3.1). These resulting values are converted into a logarithmic scale and stored in an array $\dot{\omega}_{rel_{log}}$.

$$\dot{\omega}_{rel_{log}j} = log_{10}\left(\frac{|\dot{\omega}_j|}{\dot{\omega}_{small}}\right) \quad \text{for} \quad \dot{\omega}_j \neq 0 \tag{3.1}$$

where

$$\dot{\omega}_{small} = min\left(|\dot{\omega}_j|\right) \quad \text{for} \quad \dot{\omega}_j \neq 0 \tag{3.2}$$

The maximum value, $dQ_{rel_{log}max}$, is chosen from this array and is then adjusted by η to determine the threshold for selecting QSS species. Species with values, from $dQ_{rel_{log}}$, falling below this threshold are classified as QSS species, as represented in Equation (3.3).

$$QSS_{status_i} = \begin{cases} true & \text{for} \quad \dot{\omega}_{rel_{log}j} < \eta\dot{\omega}_{rel_{log}max}, \\ false & \text{for} \quad \dot{\omega}_{rel_{log}j} \geq \eta\dot{\omega}_{rel_{log}max}, \\ true & \text{for} \quad \dot{\omega}_j = 0 \end{cases} \tag{3.3}$$

where

$$\dot{\omega}_{rel_{log}max} = max\left(\dot{\omega}_{rel_{log}(1\rightarrow N_s)}\right) \tag{3.4}$$

3.1.4 Global Adaptive Time Stepping

Time steps are limited to prevent any species concentrations from becoming negative. Equation (3.5) is evaluated for all grid cells, where ζ is a Time Step Relaxation Factor and the smallest value is chosen as the global time step.

$$\delta t = \zeta \quad min\left(\left(-\frac{C_j}{\dot{\omega}_j}\right)\right) \quad \forall \quad \dot{\omega}_j < 0 \tag{3.5}$$

3.2 HYP Code

HYP CFD code, developed by Dr. Eric Perrell [8], is a 3D-RANS solver using Steger-Warming Flux Vector Splitting and Wilcox-2006 k-Ω Turbulence Model with the capability to use both explicit and implicit methods, to enhance computational efficiency across multiple processors it uses MPI Parallelization. However, for this study, HYP will be run as a pseudo-1D RANS solver using explicit schemes with no turbulence modelling.

4 Verification

In the verification section of this thesis, the algorithm is tested to demonstrate its efficacy. The verification process utilizes a Hydrogen-Air chemistry model, specifically employing the Evans and Schexnayder 12 Species 25 Reaction model, which includes nitrogen based reactions. The algorithm's performance is assessed through simulations conducted in a simplified 1D channel with a premixed flow setup.

4.1 Chemistry Modelling

The Evans and Schexnayder Hydrogen-Air chemistry model [1], a comprehensive model of 25 reactions, is utilized for validation. This model has been further simplified into two reduced sets, one with 8 reactions and another with 16 reactions. Detailed information of their Arrhenius coefficients and Chaperon collision efficiencies [9] are provided in Table 4.1. By employing these three sets, the study aims to investigate how the complexity of the system affects the effectiveness of OTF-QSSA.

Table 4.1 Evans and Schexnayder Hydrogen Air Reaction Model [1]

No.	Reaction	A (mole, cm^3, sec)	n	$\frac{E_A}{R_u}$ (K)
1	$H_2 + M \rightarrow 2H + M$	5.5E+18	-1.0	51987.0
		1.8E+18	-1.0	0.0
2	$O_2 + M \rightarrow 2O + M$	7.2E+18	-1.0	59340.0
		4.0E+17	-1.0	0.0
3	$H_2O + M \rightarrow OH + H + M$	5.2E+21	-1.5	59386.0
		4.4E+20	-1.5	0.0
4	$OH + M \rightarrow O + H + M$	8.5E+18	-1.	50830.0
		7.1E+18	-1.0	0.0
5	$H_2O + O \rightarrow 2OH$	5.8E+13	0.0	9059.0
		5.3E+12	0.0	503.0

Table 4.1 continued

No.	Reaction	A (mole, cm^3, sec)	n	$\frac{E_A}{R_u}$ (K)
6	$H_2O + H \rightarrow OH + H_2$	8.4E+13	0.0	10116.0
		2.0E+13	0.0	2600.0
7	$O_2 + H \rightarrow OH + O$	2.2E+14	0.0	8455.0
		1.5E+13	0.0	0.0
8	$H_2 + O \rightarrow OH + H$	7.5E+13	0.0	5586.0
		3.0E+13	0.0	4429.0
9	$H_2 + O_2 \rightarrow 2OH$	1.7E+13	0.0	24232.0
		5.7E+11	0.0	14922.0
HO_2 Reactions				
10	$HO_2 + M \rightarrow H + O_2 + M$	1.7E+16	0.0	23100.0
		1.1E+16	0.0	-440.
11	$H_2 + O_2 \rightarrow H + HO_2$	1.9E+13	0.5	24100.0
		1.3E+13	0.0	0.0
12	$2OH \rightarrow H + HO_2$	1.7E+11	0.5	21137.0
		6.0E+13	0.0	0.0
13	$H_2O + O \rightarrow H + HO_2$	5.8E+11	0.5	28686.0
		3.0E+13	0.0	0.0
14	$OH + O_2 \rightarrow O + HO_2$	3.7E+11	0.64	27840.0
		1.0E+13	0.0	0.0
15	$H_2O + O_2 \rightarrow OH + HO_2$	2.0E+11	0.5	36296.0
		1.2E+13	0.0	0.0
16	$H_2O + OH \rightarrow H_2 + HO_2$	1.2E+12	0.21	39815.0
		1.7E+13	0.0	12582.0

Table 4.1 continued

No.	Reaction	A (mole, cm^3, sec)	n	$\frac{E_A}{R_u}$ (K)
N_2 Reactions				
17	$HNO_2 + M \rightarrow NO + OH + M$	5.0E+17	-1.0	25000.0
		8.0E+15	0.0	-1000.0
18	$NO_2 + M \rightarrow NO + O + M$	1.1E+16	0.0	32712.0
		1.1E+15	0.0	-941.0
19	$O + N_2 \rightarrow N + NO$	5.0E+13	0.0	37940.0
		1.1E+13	0.0	0.0
20	$H + NO \rightarrow N + OH$	1.7E+14	0.0	24500.0
		4.5E+13	0.0	0.0
21	$O + NO \rightarrow N + O_2$	2.4E+11	0.5	19200.0
		1.0E+12	0.5	3120.0
22	$NO + OH \rightarrow H + NO_2$	2.0E+11	0.5	15500.0
		3.5E+14	0.0	740.0
23	$NO + O_2 \rightarrow O + NO_2$	1.0E+12	0.0	22800.0
		1.0E+13	0.0	302.0
24	$NO_2 + H_2 \rightarrow H + HNO_2$	2.4E+13	0.0	14500.0
		5.0E+11	0.5	1500.0
25	$NO_2 + OH \rightarrow NO + HO_2$	1.0E+11	0.5	6000.0
		3.0E+12	0.5	1200.0

First 8 reactions make up the 8 Reaction Model

First 16 reactions make up the 16 Reaction Model

For every reaction: 1^{st} row represents forward; 2^{nd} row represents backward rates

[M] = 2.5[H_2]+16.25[H_2O]+1[Others] [9]

Table 4.2 Reaction Set and their Species

Case	Species	Reaction Set
1	H_2, O_2, H_2O, OH, O, H, N_2	Reactions 1 $\rightarrow$ 8
2	H_2, O_2, H_2O, OH, O, H, HO_2, N_2	Reactions 1 $\rightarrow$ 16
3	H_2, O_2, H_2O, OH, O, H, HO_2, N_2, N, HNO_2, NO, NO_2	Reactions 1 $\rightarrow$ 25

4.2 Pre-mixed 1D-Channel Flow

The validation case under consideration simulates a simple Pre-Mixed 1D channel flow of hydrogen and air, similar to that of the NPARC Alliance Validation Channel Combustion case [10]. The channel extends to a length of 5 inches, equivalent to 0.127 meters, with the computational domain being split into a 200-cell grid maintaining uniform spacing along the channel's length, as shown in Figure 4.1.

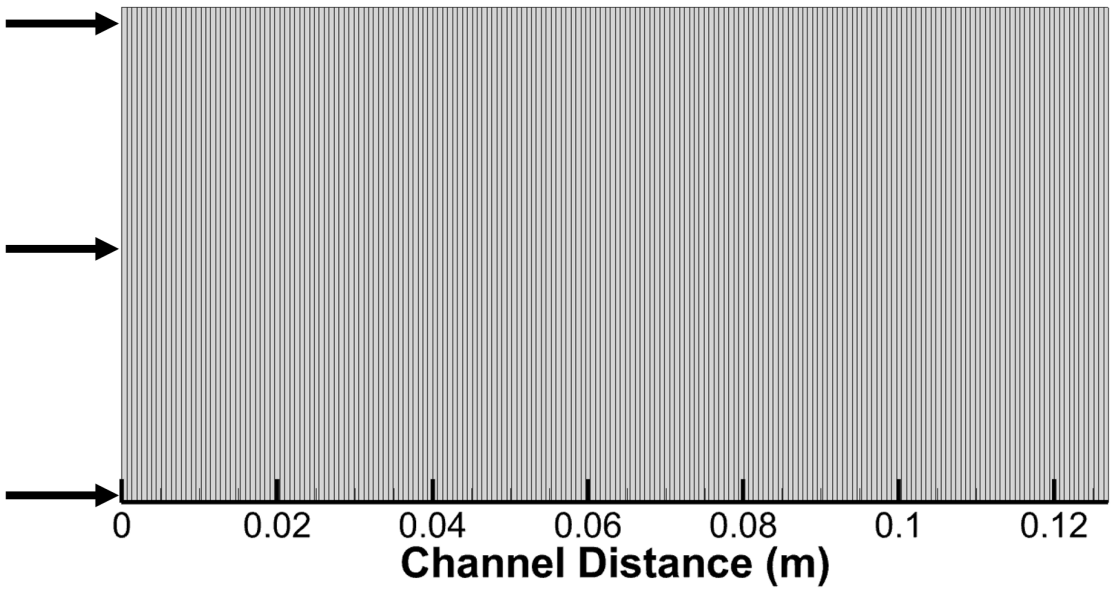

Figure 4.1 1D Channel Grid

The air within the simulation is modeled to consist solely of nitrogen and oxygen. The initial conditions at the channel inlet are listed in Table 4.4 and the inflow species mole

fractions are listed in Table 4.3.

Table 4.3 Inflow Species Mass Fractions

Species	**Mole Fractions**
H_2	0.1
O_2	0.2
N_2	0.7
H_2O	0.0
OH	0.0
H	0.0
O	0.0
HO_2	0.0
N	0.0
NO_2	0.0
NO	0.0
NO_2	0.0

Table 4.4 Inflow Conditions

Parameter	**Value**
Velocity	1359 $\frac{m}{s}$
Temperature	1389 K
Pressure	101325 Pa

5 Results and Discussion

This section presents the analysis of pre-mixed 1D channel flow simulations using the Evans and Schexnayder Full Chemistry Model and its derivatives. The comparative study, between the detailed version as well as between the 3 cases themselves, aims to evaluate the OTF-QSSA's feasibility in reducing the computational requirements that are needed to solve chemical kinetics.

5.1 Case 1: Evans and Schexnayder 7 Species - 8 Reactions

For examining the Evans and Schexnayder 8-Reaction model, a Courant-Friedrichs-Lewy (CFL) number of 0.4 was maintained throughout 4,000 iterations. The QSSA Relaxation Factor (η) was set at 0.4. The Concentration Update Count (ϵ_u) was fixed at 5, meaning the concentrations of QSS species were updated every 5 iterations and the QSSA Check Count (ϵ_c) was set to 10, with the status of species as QSS were re-evaluated every 50 iterations. For this case, the QSSA was enabled downstream of the channel at 40% of its total length (Table 5.1). The OTF-QSSA enabled simulations were compared with their detailed kinetics counterparts based on mass fractions of major and minor species (Figures 5.1 and 5.2), temperature , pressure , and X-velocity profiles (Figures 5.3 - 5.5).

Table 5.1 User Constraints: Evans and Schexnayder 8 Reactions Model

Parameter	**Value**
CFL	0.4
Max Iterations	4000
η	0.2
ϵ_u	5
ϵ_c	10

For all five plots, both the OTF-QSSA enabled and the detailed models, closely aligned with each other, indicating that the application OTF-QSSA did not introduce any significant errors in the final results. Figures 5.6 and 5.7 provides the RRMSE in percentage.

There is a clear lack of potential QSS species with the 8-reaction model. Nitrogen (N_2) and hydrogen atom (H) were the only two species found to be consistently identified, in figure

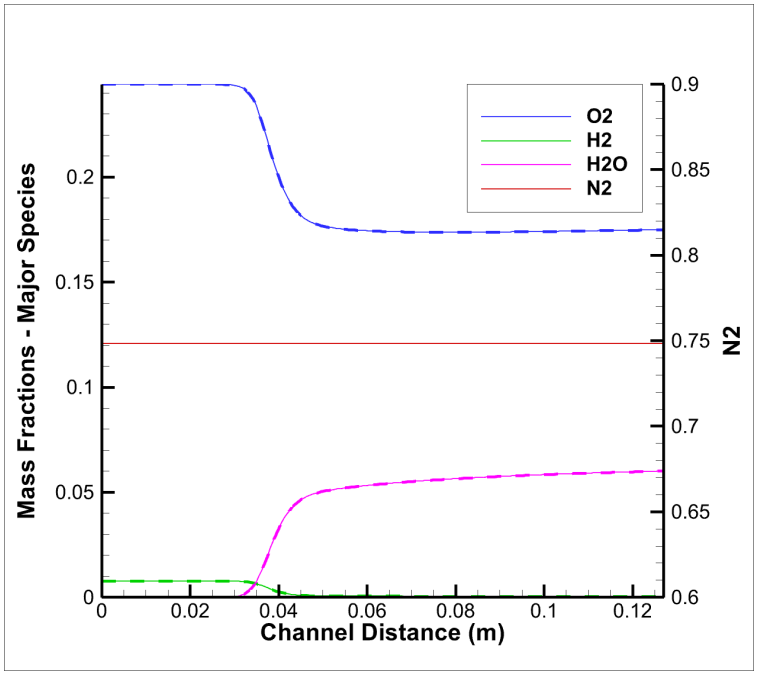

Figure 5.1 Evans and Schexnayder 7 Species - 8 Reactions Model: Major Species Mass Fractions (Dashed Lines - Without QSSA, Solid Line - With QSSA)

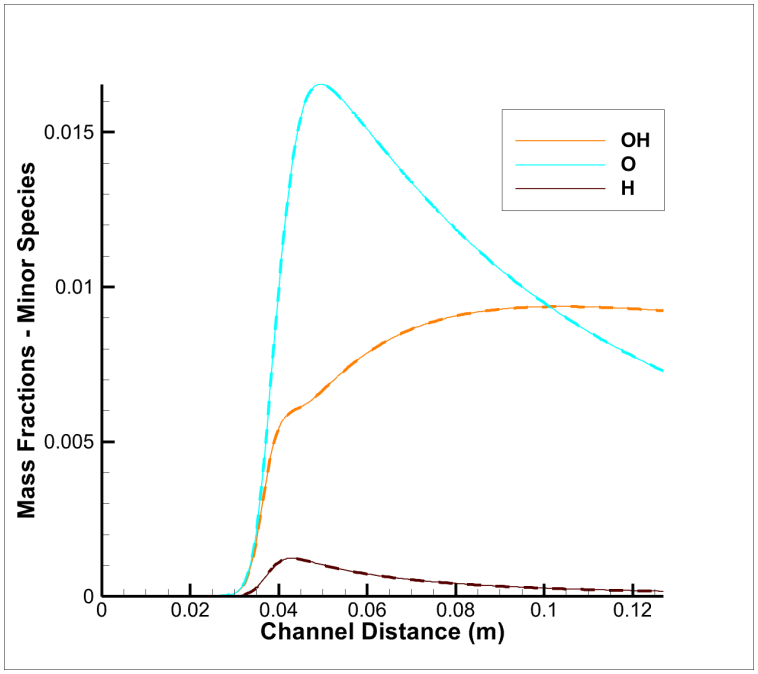

Figure 5.2 Evans and Schexnayder 7 Species - 8 Reactions Model: Minor Species Mass Fractions (Dashed Lines - Without QSSA, Solid Line - With QSSA)

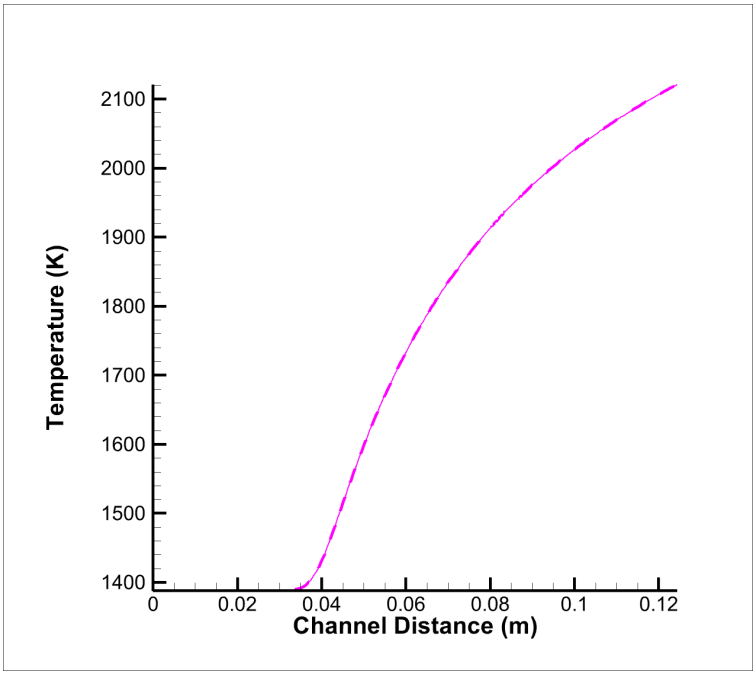

Figure 5.3 Evans and Schexnayder 7 Species - 8 Reactions Model: Temperature Dashed Lines - Without QSSA, Solid Line - With QSSA)

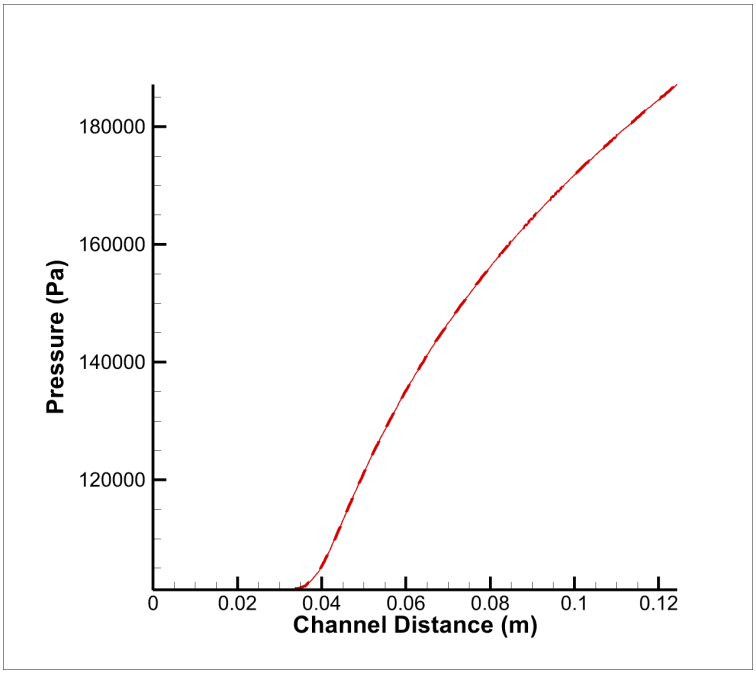

Figure 5.4 Evans and Schexnayder 7 Species - 8 Reactions Model: Pressure (Dashed Lines - Without QSSA, Solid Line - With QSSA)

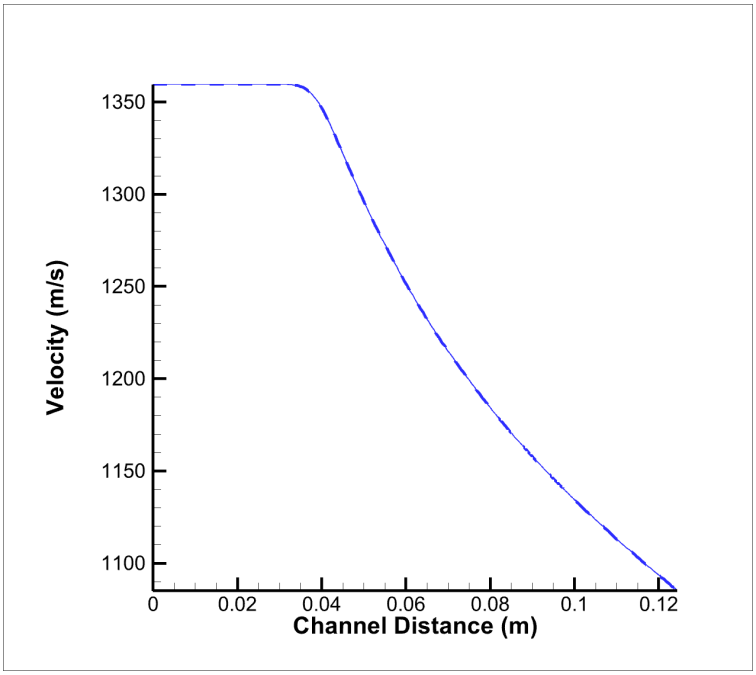

Figure 5.5 Evans and Schexnayder 7 Species - 8 Reactions Model: X-Velocity (Dashed Lines - Without QSSA, Solid Line - With QSSA)

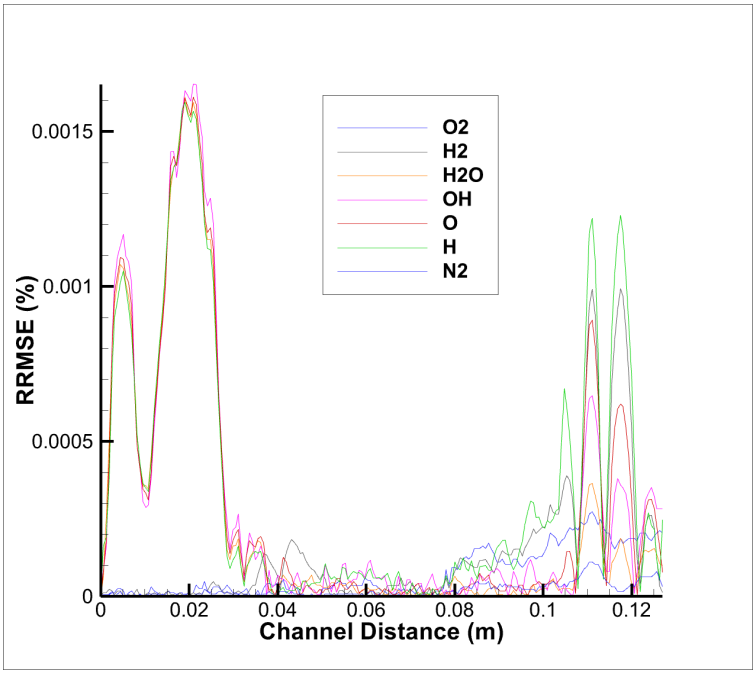

Figure 5.6 Evans and Schexnayder 7 Species - 8 Reactions Model: RRMSE Of Composition (Dashed Lines - Without QSSA, Solid Line - With QSSA)

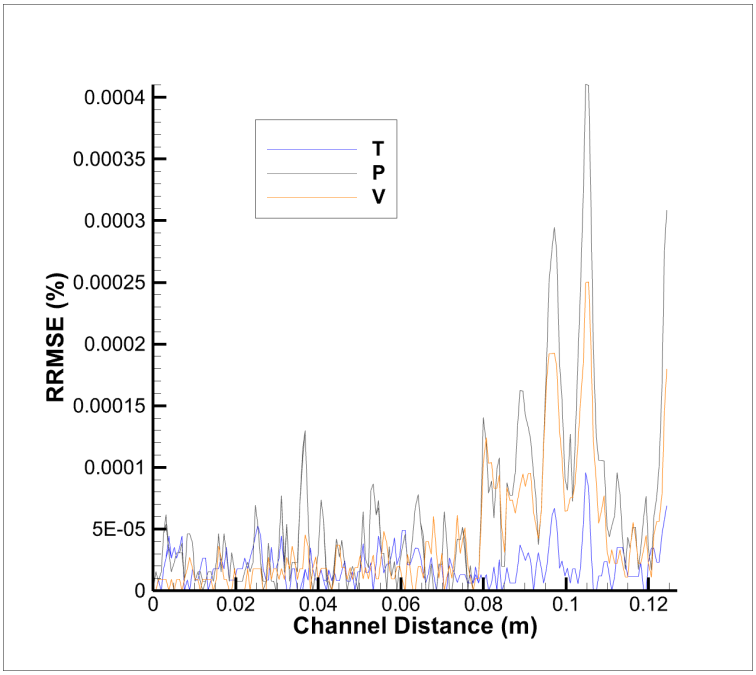

Figure 5.7 Evans and Schexnayder 7 Species - 8 Reactions Model: RRMSE Of State and Velocity (Dashed Lines - Without QSSA, Solid Line - With QSSA)

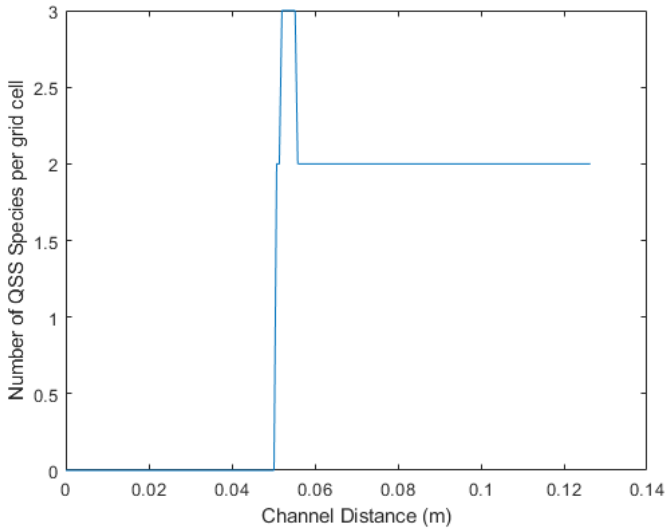

Figure 5.8 Evans and Schexnayder 7 Species - 8 Reactions Model: Average Number of QSS Species per grid cell

5.8, as a QSS species. For all other species, the rate changes were within a comparable range rendering the application of OTF-QSSA invalid. N_2 behaviors is as expected due to it not actively participating in any of the eight reactions within the model. Hence, the QSSA only really enhances the performance of H calculations and this is not enough to overcome the inherent overhead processes needed to run the QSSA algorithm which can be noticed from the poor performance of the OTF-QSSA enabled version running at 9.279 seconds, -2.41% slower compared to the detailed mechanism which completed the case in 9.061 seconds.

5.2 Case 2: Evans and Schexnayder 8 Species - 16 Reactions

For the Evans and Schexnayder 16-reaction model 2 different cases, one starting OTF-QSSA at the 1^{st} grid cell and the other starting it downstream of the channel at 40% of its total length, or 80^{th} grid cell. A η of 0.2 is chosen for both cases and were run at a CFL number of 0.1 maintained throughout a total of 50,000 iterations. ϵ_u was fixed at 5, meaning the concentrations of QSS species were updated every 5 iterations. Whereas ϵ_c was set to 200, fixing the status of species as QSS to be re-evaluated every 1000 iterations (Table 5.2).

Table 5.2 User Constraints: Evans and Schexnayder 16 Reactions Model

Parameter	**Value**
CFL	0.1
Max Iterations	50000
η	0.2
ϵ_u	5
ϵ_c	200

The OTF-QSSA case where its enabled at the first grid point showed a spatial displacement in the values as seen in figures 5.9 through 5.13. The other case, however, matched exactly with the detailed mechanism in terms of mass fractions, temperature, pressure and velocity. This spatial displacement is caused due to the incorrect assumption of some species as QSS near the early stages of the process, as seen in figure 5.14. Thus, delaying the formation of some vital radicals to start or accelerate the chemical reactions.

Hydroperoxyl (HO_2) and N_2 were consistently identified as QSS, hydrogen (H_2) and

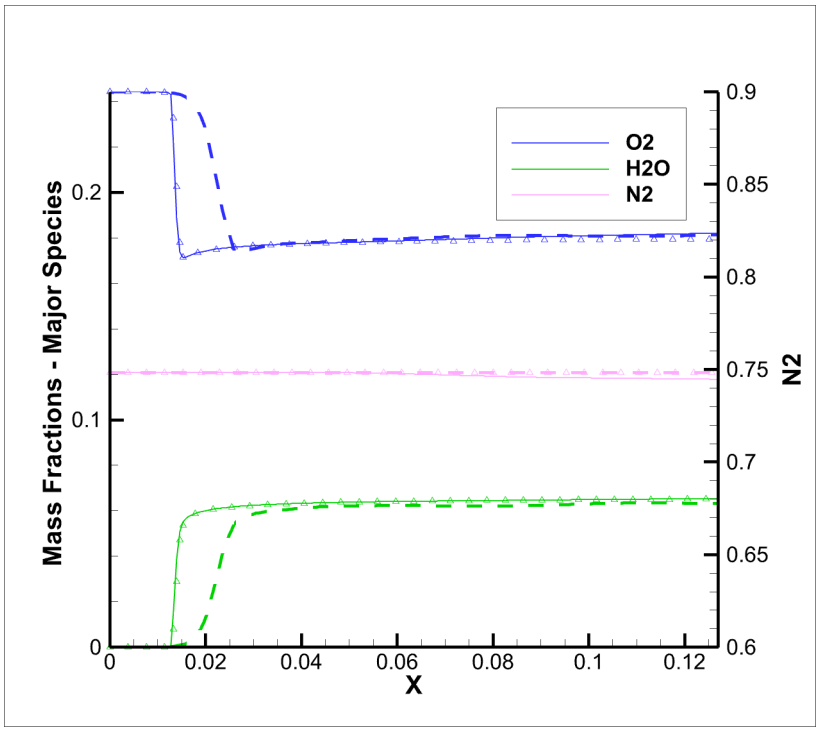

Figure 5.9 Evans and Schexnayder 8 Species - 16 Reactions Model: Major Species Mass Fractions (Dashed Lines - Without QSSA, Solid Line - With QSSA)

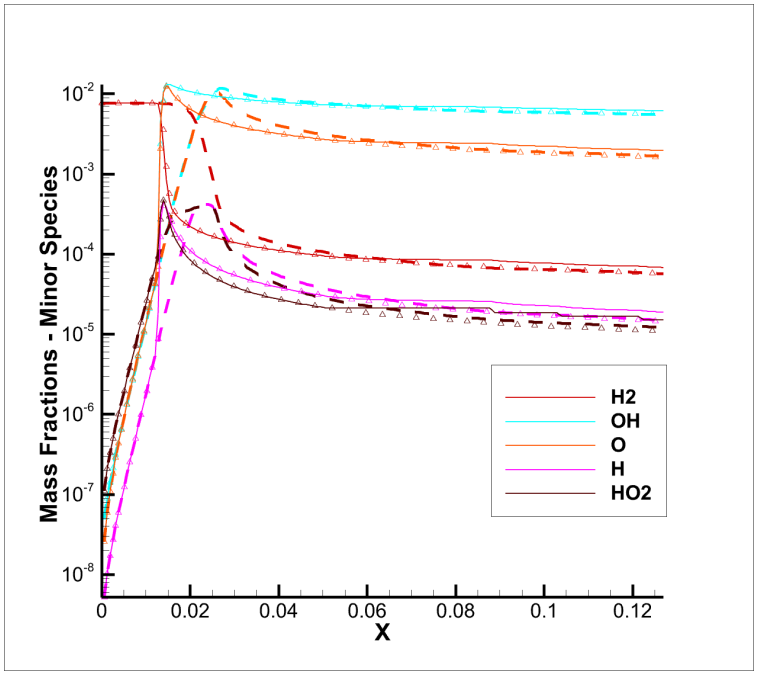

Figure 5.10 Evans and Schexnayder 8 Species - 16 Reactions Model: Minor Species Mass Fractions (Dashed Lines - Without QSSA, Solid Line - With QSSA)

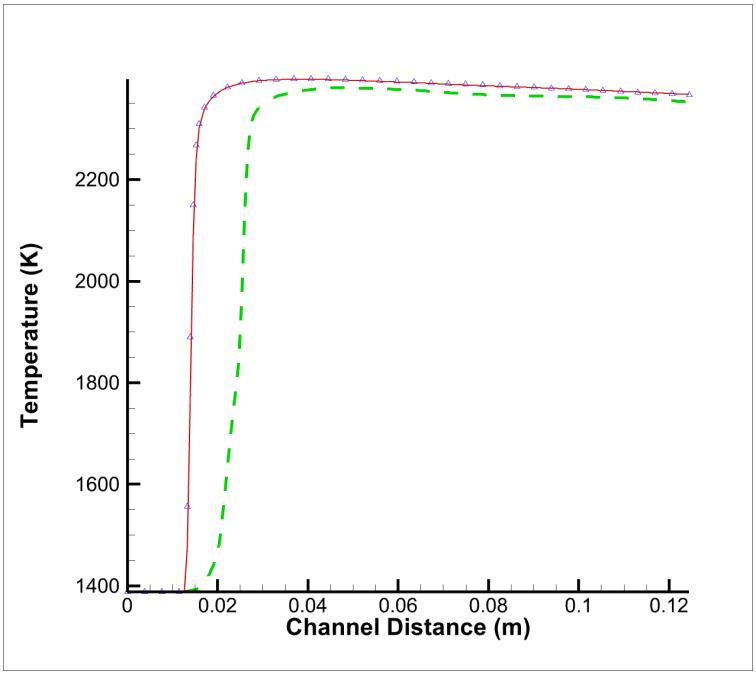

Figure 5.11 Evans and Schexnayder 8 Species - 16 Reactions Model: Temperature (Dashed Lines - Without QSSA, Solid Line - With QSSA)

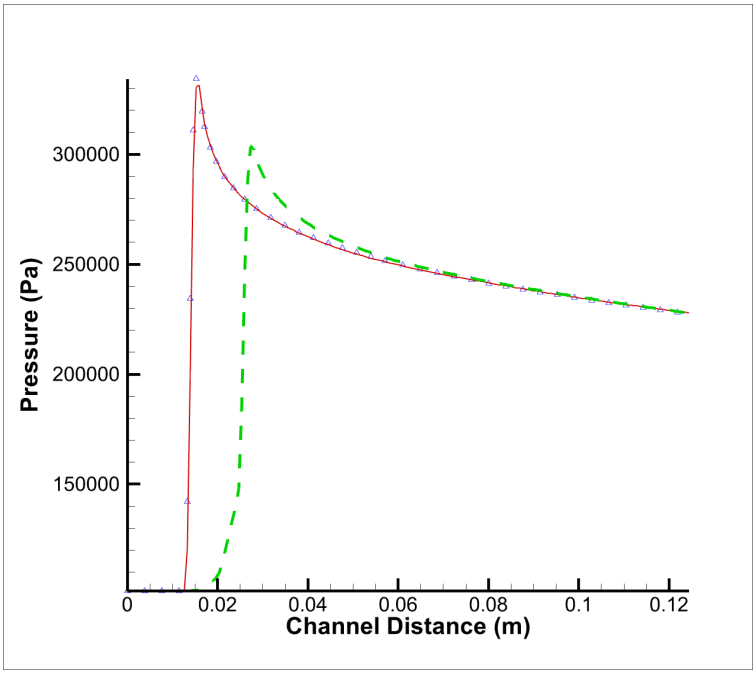

Figure 5.12 Evans and Schexnayder 8 Species - 16 Reactions Model: Pressure (Dashed Lines - Without QSSA, Solid Line - With QSSA)

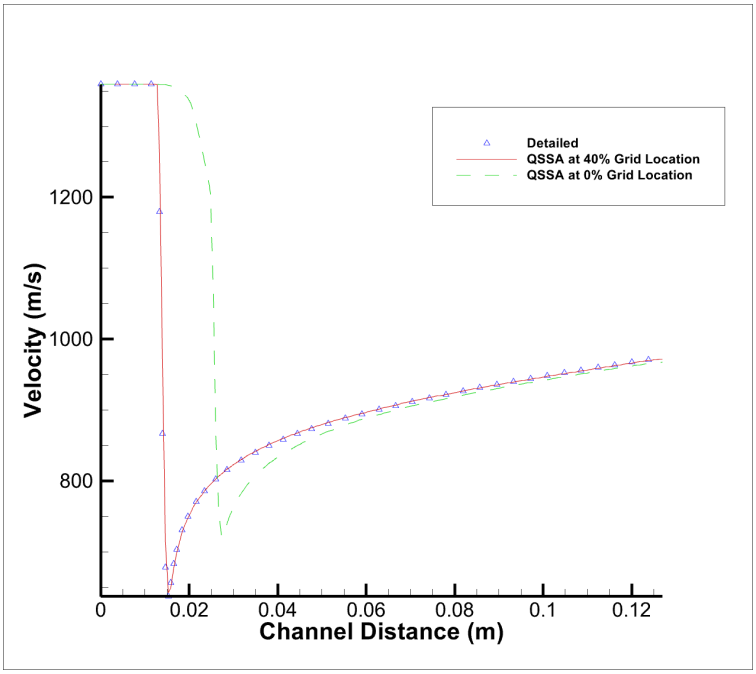

Figure 5.13 Evans and Schexnayder 8 Species - 16 Reactions Model: X-Velocity (Dashed Lines - Without QSSA, Solid Line - With QSSA)

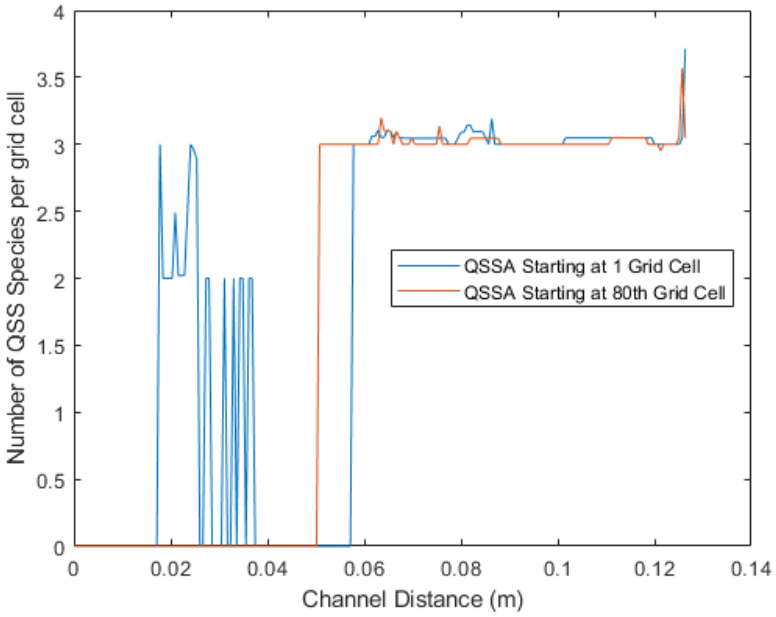

Figure 5.14 Evans and Schexnayder 8 Species - 16 Reactions Model: Average Number of QSS Species per grid cell

hydrogen atom (H) transitioned in and out of QSS status at different points during the simulation. The weighted average number of QSS species per grid cell throughout the simulation is documented in (Figure 5.14).

Computational performance wise the detailed mechanism ran for 135.533 seconds. The case where OTF-QSSA was enabled at the 1^{st} grid cell ran for 129.163 seconds, and the other ran for 130.142 seconds. A 4.70% and a 3.98% improvement compared to detailed mechanism respectively.

5.3 Case 3: Evans and Schexnayder 12 Species - 25 Reactions

For examining the 25-reaction Evans and Schexnayder model 2 different cases, one starting OTF-QSSA at the 1^{st} grid cell and the other starting it downstream of the channel at 40% of its total length, or 80^{th} grid cell, were tested. A η of 0.6 is chosen for both cases and were run at a CFL number of 0.05 maintained throughout 100,000 iterations. ϵ_u was fixed at 5, meaning the concentrations of QSS species were updated every 50 iterations and ϵ_c was set to 200, fixing the status of species as QSS to be re-evaluated every 1000 iterations. These constraints are listed in Table 5.3

Table 5.3 User Constraints: Evans and Schexnayder 25 Reactions Model

Parameter	**Value**
CFL	0.05
Max Iterations	100000
η	0.6
ϵ_u	5
ϵ_c	200

Detailed mechanism and both the OTF-QSSA enabled cases showed no discrepancies in their major and minor species mass fractions, figures 5.15 and 5.16. However, there were some noticeable differences in mass fractions of nitrogen based trace species as seen in Figure 5.17 with the OTF-QSSA case where it is enabled at the beginning of the channel showing a larger error, multiple orders of magnitude, figure 5.18. The other OTF-QSSA showed a improved accuracy when predicting mass fractions of QSS species, while it still being

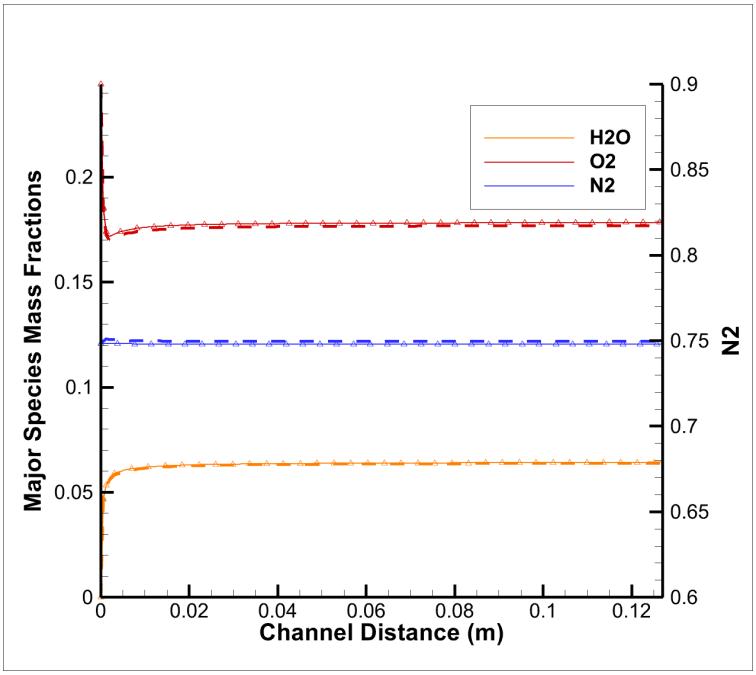

Figure 5.15 Evans and Schexnayder 12 Species - 25 Reactions Model: Major Species Mass Fractions *(Delta - Without QSSA, Dashed Lines - QSSA Case a, Solid Line - With QSSA Case b)*

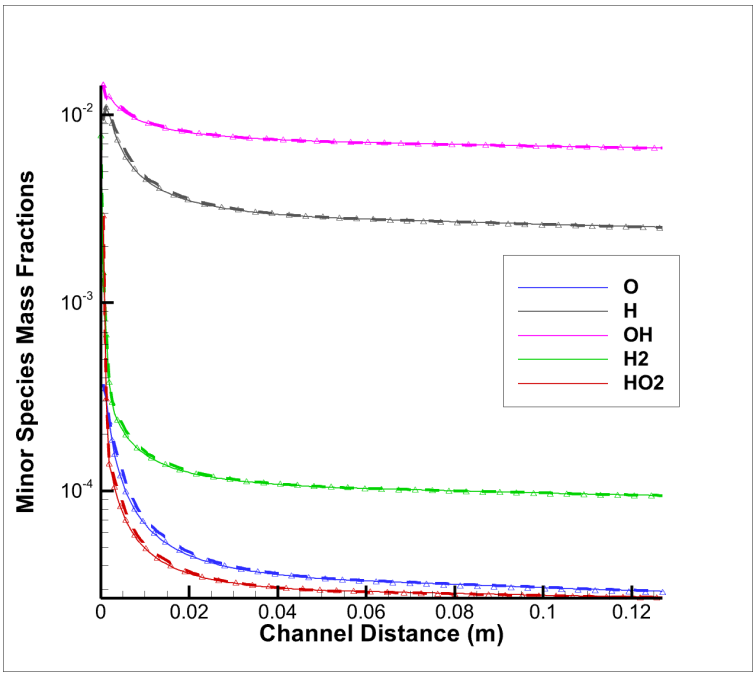

Figure 5.16 Evans and Schexnayder 12 Species - 25 Reactions Model: Minor Species (Excluding Nitrogen Based Species) Mass Fractions (Delta - Without QSSA, Dashed Lines - QSSA Case a, Solid Line - With QSSA Case b)

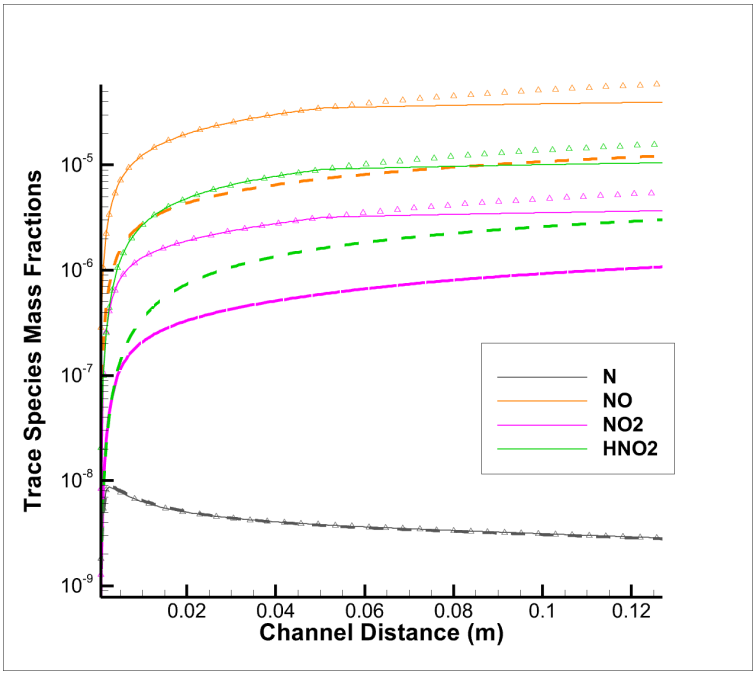

Figure 5.17 Evans and Schexnayder 12 Species - 25 Reactions Model: Minor Nitrogen Based Species Mass Fractions (Delta - Without QSSA, Dashed Lines - QSSA Case a, Solid Line - With QSSA Case b)

noticeably larger at a peak difference of 34% as shown in figure 5.19. Figures 5.22 and 5.23 show the RRMSE % error for the state and velocity values. Unlike the 16-reaction model, there were no noticeable differences in values spatially. This could be due to the relativistic nature of the algorithm when choosing QSS species. Nitrogen-based species along with HO_2 frequently emerged as QSS for the 25-reaction model whereas for the 16-reaction model species such as H and H2 were also assumed and may have been vital for the progressions of the chemical reaction. (Figure 5.27) represents the weighted average number of QSS species per grid cell for the 25-reaciton model to better visualize how species species were considered or not along the length of the grid.

The detailed simulations required 497.502 seconds to run, whereas the OTF-QSSA simulations were completed in 431.885, for the first grid cell activation case, and 437.505 seconds, for the 80^{th} grid cell activation case, resulting a substantial reduction of about 13.19% and 12.06% in computational time respectively.

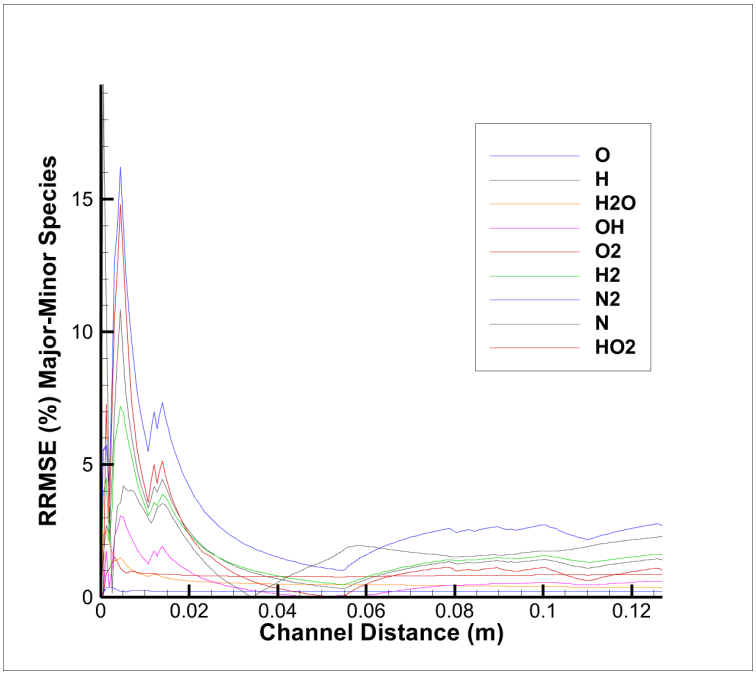

Figure 5.18 Evans and Schexnayder 12 Species - 25 Reactions Model: RRMSE (%) Major-Minor Species (Excluding Nitrogen Based Species) Mass Fractions with OTF-QSSA Enabled at 1^{st} Grid Cell

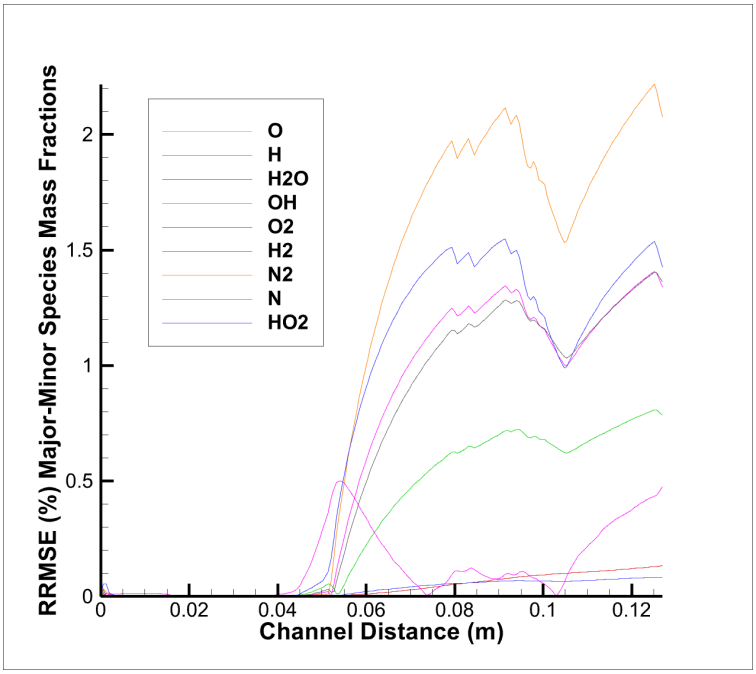

Figure 5.19 Evans and Schexnayder 12 Species - 25 Reactions Model: RRMSE (%) Major-Minor Species *(Excluding Nitrogen Based Species)* Mass Fractions with OTF-QSSA Enabled at 80^{th} Grid Cell

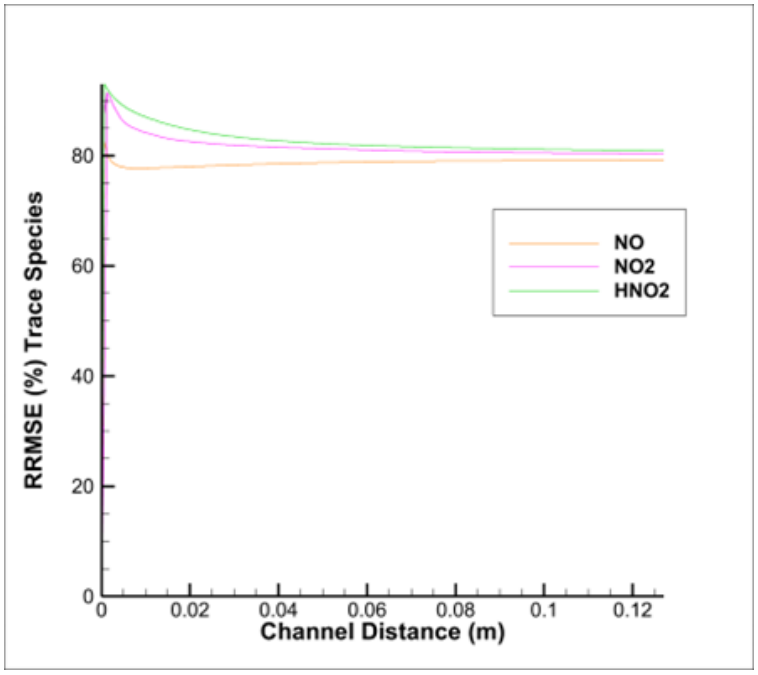

Figure 5.20 Evans and Schexnayder 12 Species - 25 Reactions Model: RRMSE (%) Nitrogen Based Trace Species Mass Fractions with OTF-QSSA Enabled at 1^{st} Grid Cell

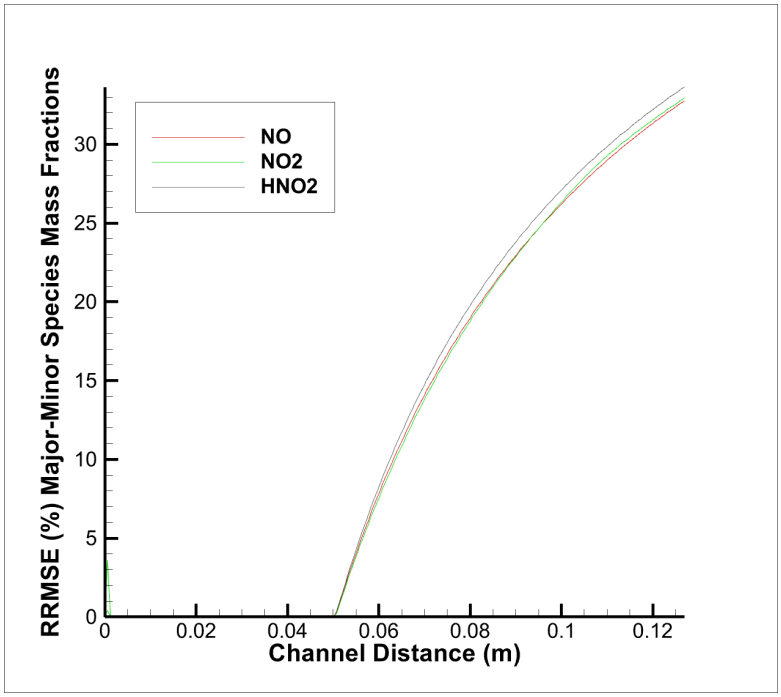

Figure 5.21 Evans and Schexnayder 12 Species - 25 Reactions Model: RRMSE (%) Nitrogen Based Trace Species Mass Fractions with OTF-QSSA Enabled at 80^{th} Grid Cell

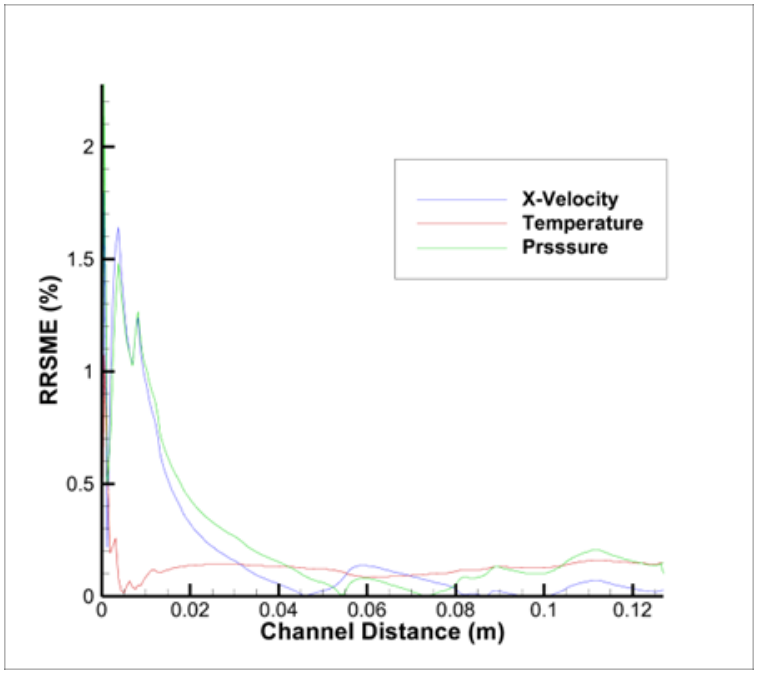

Figure 5.22 Evans and Schexnayder 12 Species - 25 Reactions Model: RRMSE (%) Of State and Velocity with OTF-QSSA Enabled at 1^{st} Grid Cell

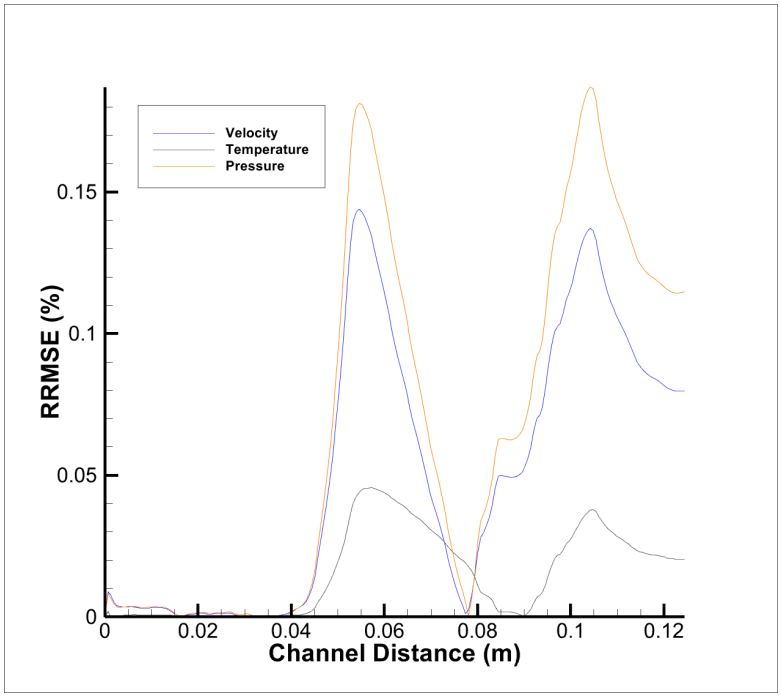

Figure 5.23 Evans and Schexnayder 12 Species - 25 Reactions Model: RRMSE (%) Of State and Velocity with OTF-QSSA Enabled at 80^{th} Grid Cell

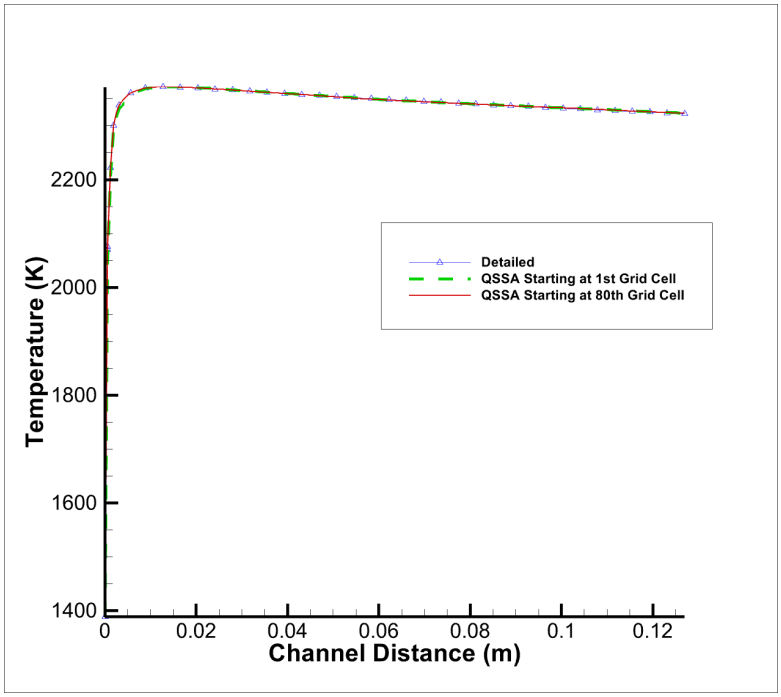

Figure 5.24 Evans and Schexnayder 12 Species - 25 Reactions Model: Temperature (Delta - Without QSSA, Dashed Lines - QSSA Case a, Solid Line - With QSSA Case b)

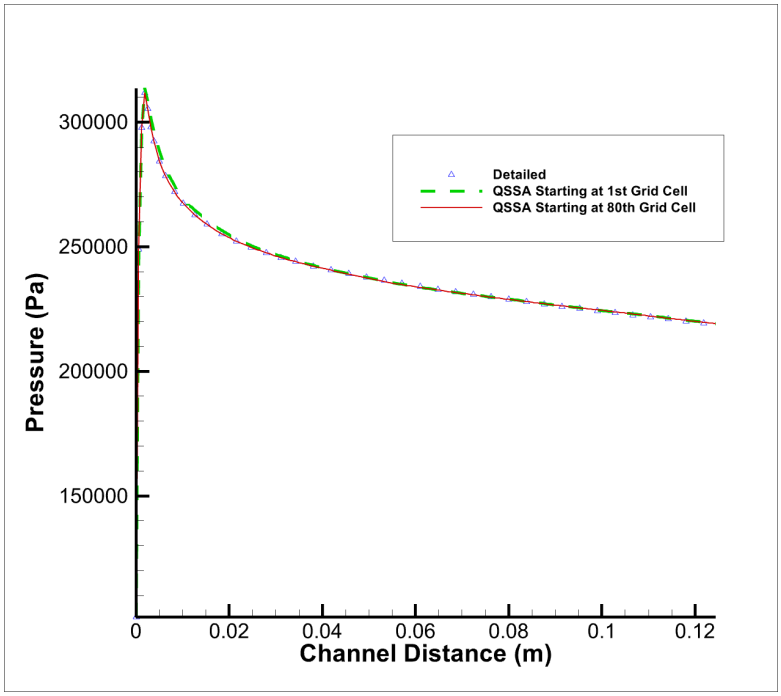

Figure 5.25 Evans and Schexnayder 12 Species - 25 Reactions Model: Pressure (Delta - Without QSSA, Dashed Lines - QSSA Case a, Solid Line - With QSSA Case b)

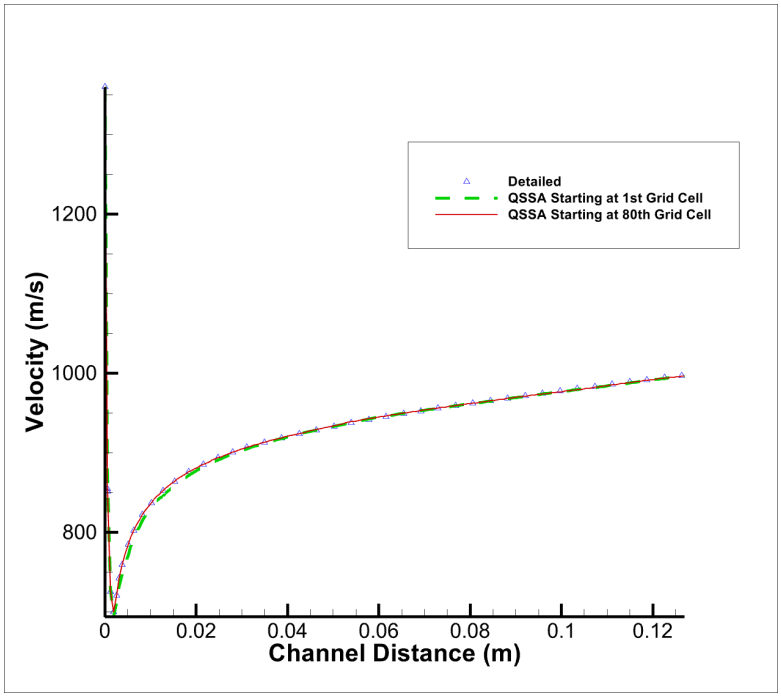

Figure 5.26 Evans and Schexnayder 12 Species - 25 Reactions Model: Velocity (Delta - Without QSSA, Dashed Lines - QSSA Case a, Solid Line - With QSSA Case b)

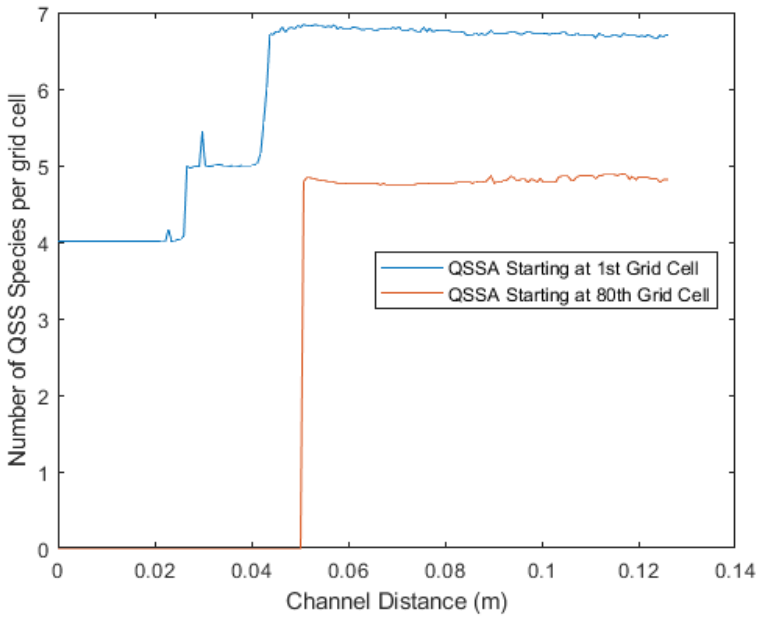

Figure 5.27 Evans and Schexnayder 12 Species - 25 Reactions Model: Average Number of QSS Species at a grid cell

6 Conclusion

6.1 Remarks

The evaluation of the OTF-QSSA using the Evans and Schexnayder model and its derivatives—encompassing 8, 16, and 25 reactions—provides insightful data on computational efficiency and accuracy across the varying complexities. The 8-reaction model exhibited an increase in computational time, indicating that OTF-QSSA may not provide computational benefits in simpler or smaller reaction systems. Conversely, the 16 and 25-reaction models demonstrated significant reductions in computational time, by 3.98% and 12.06% respectively, underscoring the potential utility of OTF-QSSA in more complex scenarios.

Further analysis showed that both the 16 and 25-reaction models experienced some discrepancies in the final results when OTF-QSSA was enabled from the start of the simulations. However, these errors were minimized when the algorithm was activated only after 40% of the channel length from the inflow, effectively bypassing the initial pre-ignition and ignition phases of the reactions. This modification improved the accuracy of the results, suggesting that the pre-ignition and ignition phases may involve dynamics that the current OTF-QSSA algorithm does not adequately address.

This pattern suggests that while OTF-QSSA may not be suitable for managing the dynamics specific to the pre-ignition and ignition phases without adjustments, it can significantly enhance computational efficiency in later stages of the reaction process. For complex chemical systems, where reducing computational load is crucial, implementing OTF-QSSA beyond the initial reaction phases can lead to substantial performance improvements, thereby affirming its value as a tool for simplifying the modeling of chemical kinetics.

6.2 Limitation of the Current Model

The OTF-QSSA demonstrates limited effectiveness in simpler chemical reaction cases, primarily due to a lack of sufficient potential QSS species. This deficiency means that the computational overhead inherent in the OTF-QSSA processes is not adequately offset by efficiency gains, rendering the approach less beneficial in these scenarios. Additionally, the

algorithm currently struggles with accurately handling the complex dynamics of pre-ignition and ignition phases within the chemical reaction mechanisms. These phases often involve rapid changes in species concentrations and reaction rates that the algorithm fails to capture effectively.

To address these shortcomings, there is a clear need for a revised QSS selection methodology that can more accurately identify and utilize potential QSS species during all reaction phases. Moreover, enhancements to the time marching algorithm for QSS species should aim to provide more precise control QSS species concentration updates, ensuring that the algorithm can more effectively manage the rapid changes occurring during critical reaction stages such as pre-ignition and ignition.

REFERENCES

[1] Evans, J. S., and Schexnayder, C. J., "Influence of Chemical Kinetics and Unmixedness on Burning in Supersonic Hydrogen Flames," *AIAA Journal*, Vol. 18, No. 2, 1980, pp. 188–193. https://doi.org/10.2514/3.50747.

[2] Kuo, K. K., *Principles of Combusiton*, John Wiley, 2005.

[3] Turns, S., and Haworth, D. C., *An Introduction to Combustion: Concepts and Applications*, McGraw Hill, 2021.

[4] Zhang, S., Androulakis, I. P., and Ierapetritou, M. G., "A hybrid kinetic mechanism reduction scheme based on the on-the-fly reduction and quasi-steady-state approximation," *Chemical Engineering Science*, Vol. 93, 2013, pp. 150–162. https://doi.org/10.1016/j.ces.2013.01.066.

[5] Verwer, J. G., and Simpson, D., "Explicit methods for stiff ODEs from atmospheric chemistry," *Applied Numerical Mathematics*, Vol. 18, 1995, pp. 413–430. https://doi.org/10.1016/0168-9274(95)00068-6.

[6] Mott, D. R., Oran, E. S., and B., L., "A Quasi-Steady-State Solver for the Stiff Ordinary Differential Equations of Reaction Kinetics," *Journal of Computational Physics*, Vol. 164, 2000, pp. 407–428. https://doi.org/10.1006/jcph.2000.6605.

[7] Lu, T., and Law, C. K., "Systematic Approach To Obtain Analytic Solutions of Quasi Steady State Species in Reduced Mechanisms," *The Journal of Physics Chemistry A*, Vol. 110, No. 49, 2006, pp. 13202–13208. https://doi.org/10.1021/jp064482y.

[8] Perrell, E. R., "Computation of Combustion Heated Hypersonic Wind Tuneel Flows in Phase Nonequilibrium," Ph.D. thesis, North Carolina State University, Raleigh, North Carolina, United States of America, 1994.

[9] Bhagwandin, V., W., E., and N., G., "Numerical Simulation of a Hydrogen-Fueled Dual-Mode Scramjet Engine Using Wind-US," *45th AIAA/ASME/SAE/ASEE Joint Propulsion Conference & Exhibit*, 2009. https://doi.org/10.2514/6.2009-5382.

[10] "Hydrogen-Air Combustion in a Channel," , 2021. https://doi.org/https://www.grc.nasa.gov/WWW/wind/valid/channel.html.

[11] Peters, N., and Rogg, B., *A Reduced Kinetic Mechanisms for Applications in Combustion Systems*, Springer, 2008. https://doi.org/10.1007/978-3-540-47543-9.